

STRIDE: Scalable and Interpretable XAI via Subset-Free Functional Decomposition

Chaeyun Ko

Department of Mathematics, Ewha Womans University, Seoul, South Korea

chaeyuniris@gmail.com

linkedin.com/in/chaeyunko

Abstract

Most explainable AI (XAI) frameworks face two practical limitations: the exponential cost of reasoning over feature subsets and the reduced expressiveness of summarizing effects as single scalar values. We present STRIDE, a scalable framework that aims to mitigate both issues by framing explanation as a *subset-enumeration-free*, orthogonal functional decomposition in a Reproducing Kernel Hilbert Space (RKHS). Rather than focusing only on scalar attributions (ϕ_i), STRIDE computes functional components $f_S(x_S)$ via an analytical projection scheme based on a recursive kernel-centering procedure, avoiding explicit subset enumeration. In the tabular setups we study, the approach is model-agnostic, provides both local and global views, and is supported by theoretical results on orthogonality and L^2 convergence under stated assumptions. On public tabular benchmarks in our environment, we observed speedups ranging from $0.6\times$ (slower than TreeSHAP on a small dataset) to $9.7\times$ (California), with a median $\approx 3.0\times$ across 10 datasets, while maintaining high fidelity (R^2 between 0.81 and 0.999) and substantial rank agreement on most datasets. Overall, STRIDE complements scalar attribution methods by offering a structured functional perspective, enabling novel diagnostics like ‘component surgery’ to quantitatively measure the impact of specific interactions within our experimental scope.

Index Terms

Explainable Artificial Intelligence (XAI), Scalable Explainability, Orthogonal Decomposition, Feature Interaction, Kernel Methods, Shapley Value, Reproducing Kernel Hilbert Space (RKHS)

I. INTRODUCTION

AS machine learning models grow more complex, interpreting their decision-making processes remains a core challenge in explainable artificial intelligence (XAI). While deep neural networks and ensemble methods achieve remarkable predictive accuracy, their black-box nature hinders trust and scientific interpretability. This has led to a proliferation of feature attribution methods, but they are often constrained by fundamental limitations.

First, methods grounded in Shapley values [2], while axiomatically fair, face the exponential complexity (2^d) of evaluating all feature subsets, forcing practitioners to rely on slow sampling approximations like KernelSHAP. In parallel, surrogate-based explanation techniques such as LIME [1] approximate local decision boundaries with simpler models, but often lack global consistency. Second, even highly optimized, model-specific methods like TreeSHAP [13], neural network approaches like Integrated Gradients [14] or DeepLIFT [15], are limited in expressiveness: they distill the rich, non-linear effect of a feature into a **single scalar value** (ϕ_i). This answers *what* features are important but provides less insight into *how* they form complex, non-additive interactions. Third, prior attempts at functional decomposition have been largely restricted to global-only analysis [4] or specific model classes [6], limiting general applicability.

We introduce **STRIDE** (Subset-free Kernel-Based Decomposition for Explainable AI), a framework that aims to mitigate these limitations. STRIDE reframes model explanation as a **model-agnostic, instance-specific functional decomposition** in the tabular setups we study. Using a recursive centering of product kernels in an RKHS, it computes orthogonal contribution functions $f_S(x_S)$ for feature subsets S via an analytical projection scheme, without explicitly enumerating subsets. In our studies, this procedure was computationally efficient within scope and expressive in revealing functional structure for the tested models.

The key contributions of this paper are:

Work primarily conducted during M.S. program at Ewha Womans University.

- We present a framework that moves beyond scalar attributions by recovering orthogonal functional components, providing a richer, more structured view of model behavior.
- We develop a subset-enumeration-free procedure based on recursively centered kernels that computes the decomposition via analytical projections, reducing the combinatorial overhead of traditional approaches.
- We provide theoretical results for orthogonality, uniqueness, and L^2 convergence under stated assumptions (e.g., bounded kernels and standard universality conditions).
- We empirically evaluate STRIDE on 10 public tabular datasets with multi-seed experiments; in our environment, we observed speedups ranging from $0.6\times$ to $9.7\times$ (median $\approx 3.0\times$), while maintaining high fidelity (R^2 between 0.81 and 0.999) and substantial rank agreement on most datasets.
- We demonstrate a novel analytical capability, which we term ‘component surgery,’ to isolate and quantify the performance impact of individual interaction components, revealing their functional importance to the model’s logic.

Ultimately, STRIDE offers a principled framework for analyzing learned functions through functional decomposition, complementing scalar attribution approaches and helping bridge the gap between local attribution and global functional analysis.

II. RELATED WORK

STRIDE builds upon, while differing in emphasis from, established ideas in functional analysis and game theory for interpretability. We briefly review Functional ANOVA and Reproducing Kernel Hilbert Spaces (RKHS), then discuss how related XAI lines have approached these tools and where remaining gaps motivate our formulation.

A. Foundations: Functional ANOVA and RKHS

The decomposition of a function into orthogonal components dates back to Hoeffding’s ANOVA decomposition [5]. For a square-integrable function $f : \mathcal{X} \rightarrow \mathbb{R}$, one can expand f into zero-mean subfunctions f_S indexed by subsets $S \subseteq \{1, \dots, d\}$, separating main effects from higher-order interactions with respect to a reference measure ν .

Reproducing Kernel Hilbert Spaces (RKHS) provide a Hilbert space structure for studying functions via positive-definite kernels K with the reproducing property $\langle f, K(\cdot, x) \rangle_{\mathcal{H}_K} = f(x)$ [10]. When K is universal, \mathcal{H}_K can be dense in $L^2(\mathcal{X})$ under suitable conditions [11, 12], enabling projection-based analyses.

B. Functional Decomposition in XAI

Several works adapt functional ANOVA ideas for interpretability. Durrande et al. [3] develop ANOVA kernels in an RKHS; in practice, their formulation involves marginal integration and has been primarily studied with surrogate models such as Gaussian Processes. Kernel-based global sensitivity methods (e.g., kernel Sobol indices [4]) provide informative population-level summaries but are not designed for instance-level explanations. Lengerich et al. [6] recover functional components for tree ensembles with an efficient algorithm, albeit in a model-specific setting.

Relative to these directions, STRIDE uses a recursive kernel-centering procedure intended to (i) avoid explicit marginal integration, (ii) operate post hoc on model outputs in the tabular setups we study (thus model-agnostic within this scope), and (iii) produce instance-level decompositions $f = \sum_S f_S(x_S)$ that connect local and aggregated views.

C. Shapley Values in RKHS and Their Limitations

Shapley-value methods, including SHAP [2], offer axiomatic appeal but can be challenged by the combinatorial growth of feature subsets, motivating approximations such as KernelSHAP. RKHS-SHAP [7] improves estimation for kernel methods yet focuses on scalar attributions (ϕ_i), which do not directly expose the functional form of interactions. Functional-decomposition approaches like Hiabu et al. [8] target settings with low-dimensional additive structure (e.g., GAM-like models), providing complementary insights with different assumptions.

Complementary to these lines, STRIDE aims to recover functional components $f_S(x_S)$ and, when desired, aggregate them to Shapley-compatible scalars (e.g., $\phi_i = \sum_{S \ni i} \frac{1}{|S|} f_S(x_S)$). This provides a structured view that can coexist with scalar attribution, while retaining compatibility in aggregation.

D. The Subset-Enumeration-Free Perspective

A common bottleneck for subset-based attribution and functional methods is the growth in subsets with dimensionality. Recent work (e.g., PKeX-Shapley [9]) shows polynomial-time computation under specific product-kernel expansions. Our approach takes a different route: in the version studied here, STRIDE avoids explicit subset enumeration by projecting onto an orthogonal basis of centered kernels constructed recursively. To our knowledge, this combination of subset-enumeration-free computation with post-hoc, instance-level analysis in an RKHS setting remains underexplored, and our evaluation indicates it may serve as a practical complement to existing methods within the tabular scope studied here.

E. Emerging Neural Function Approximators

Recently, Kolmogorov–Arnold Networks (KANs) [16] have been proposed as a new paradigm for learning basis functions with adaptive complexity. While their primary goal is improved representation learning rather than interpretability, their emphasis on functional decomposition resonates with our objectives. We view STRIDE as complementary: whereas KANs provide a learnable basis for function approximation, STRIDE leverages kernel-theoretic structure to produce post-hoc decompositions of black-box models.

Summary. Within the evaluated tabular scope, STRIDE contributes a post-hoc, RKHS-based functional view that (i) targets instance-level decompositions, (ii) remains compatible with scalar attributions via aggregation, and (iii) avoids explicit subset enumeration through recursive kernel centering. We view it as complementary to prior ANOVA–RKHS and Shapley-based approaches.

III. THEORETICAL FRAMEWORK

We formalize the theoretical basis of STRIDE within an $L^2(\mu)$ setting. Our construction leverages a family of *centered kernels* that induce mutually orthogonal subspaces; under stated assumptions, these subspaces can support a decomposition of f into components f_S indexed by feature subsets S . Throughout, uniqueness and orthogonality are always understood with respect to the chosen measure μ and kernel family.

A. Preliminaries and Assumptions

Let $T = \prod_{i=1}^d T_i$ be a product space with a finite product measure $\mu = \bigotimes_{i=1}^d \mu_i$. For each $i \in [d]$, let $k_i : T_i \times T_i \rightarrow \mathbb{R}$ be measurable and bounded. We assume there exists $c_i > 0$ such that

$$\int_{T_i} k_i(x_i, t_i) d\mu_i(t_i) = c_i \quad \text{for all } x_i \in T_i,$$

and define normalized base kernels $\tilde{k}_i := k_i/c_i$, which satisfy $\int_{T_i} \tilde{k}_i(x_i, t_i) d\mu_i(t_i) = 1$. For non-empty $S \subseteq [d]$, set

$$K_S(x_S, t_S) := \prod_{i \in S} \tilde{k}_i(x_i, t_i), \quad K_\emptyset \equiv 1.$$

We work with the standard $L^2(\mu)$ inner product, $\langle g, h \rangle := \int_T g(x)h(x) d\mu(x)$. Interchanges of integrals use boundedness and finiteness assumptions (Tonelli/Fubini conditions).

B. Centered Kernels and Orthogonality

We isolate the contribution of a subset S by removing all lower-order terms.

Definition 1 (Centered Subset Kernel). *For non-empty $S \subseteq [d]$, define recursively*

$$K_S^{(c)} := K_S - \sum_{R \subsetneq S} K_R^{(c)}, \quad \text{with } K_\emptyset^{(c)} := 1.$$

By inclusion–exclusion, this is equivalent to a Möbius inversion on the subset lattice.

Lemma 1 (Möbius Inversion). *For any $S \subseteq [d]$,*

$$K_S = \sum_{R \subseteq S} K_R^{(c)} \quad \text{and} \quad K_S^{(c)} = \sum_{R \subseteq S} (-1)^{|S|-|R|} K_R.$$

A key property is zero-mean along any coordinate in S .

Lemma 2 (Partial Zero-Mean). *For any non-empty $S \subseteq [d]$ and $i \in S$,*

$$\int_{T_i} K_S^{(c)}(x_S, t_S) d\mu_i(t_i) = 0.$$

Proof. By induction on $|S|$. Using $\int_{T_i} K_S d\mu_i = K_{S \setminus \{i\}}$ and Lemma 1, the lower-order terms cancel, yielding zero. \square

This yields orthogonality across distinct subsets (with respect to μ).

Theorem 1 (Orthogonality of Centered Kernels (under assumptions)). *For distinct $S, J \subseteq [d]$ and fixed anchors t_S, t_J ,*

$$\langle K_S^{(c)}(\cdot_S, t_S), K_J^{(c)}(\cdot_J, t_J) \rangle = 0.$$

Proof. Pick $i \in S \setminus J$. Since $K_J^{(c)}$ does not depend on x_i , integrate in x_i first and apply Lemma 2. \square

C. Subset- and Feature-Level Components

Let $\mathcal{H}_S := \overline{\text{span}}\{K_S^{(c)}(\cdot_S, t_S) : t_S \in T_S\} \subset L^2(\mu)$. By Theorem 1, the collection $\{\mathcal{H}_S\}_{S \subseteq [d]}$ is mutually orthogonal. Define the closed sum

$$\mathcal{H} := \overline{\bigoplus_{S \subseteq [d]} \mathcal{H}_S} \subseteq L^2(\mu).$$

Under universal-kernel conditions (and suitable support assumptions on μ), \mathcal{H} can be dense in $L^2(\mu)$; this assumption may not hold for all kernel/data choices, and our empirical implementation enforces it numerically.

Proposition 1 (Orthogonal Decomposition in \mathcal{H}). *For any $f \in \mathcal{H}$, there exist unique components $f_S \in \mathcal{H}_S$ such that*

$$f = \sum_{S \subseteq [d]} f_S, \quad \text{with} \quad f_S(x_S) = \langle f, K_S^{(c)}(\cdot_S, x_S) \rangle.$$

Proof. Existence/uniqueness follows from orthogonal projections onto the closed subspaces \mathcal{H}_S and the mutual orthogonality (Hilbert space Pythagorean theorem). \square

Finally, aggregating $\{f_S\}$ yields feature-level scalar attributions that align with Shapley axioms under the standard baseline convention.

Proposition 2 (Shapley-Compatible Aggregation). *Given $f = \sum_S f_S$ with $f_\emptyset = \mathbb{E}_\mu[f]$, define*

$$\phi_i(x) := \sum_{S \ni i} \frac{1}{|S|} f_S(x_S).$$

Then $\{\phi_i\}_{i=1}^d$ satisfies efficiency, symmetry, dummy, and linearity.

Proof. Efficiency: $\sum_i \phi_i(x) = \sum_S f_S(x_S) = f(x)$. Symmetry, dummy, and linearity follow from the definition and the linearity of inner products/aggregation. \square

Remark. In practice, all integrals are approximated numerically and projections are computed with finite samples. Orthogonality and completeness therefore hold up to numerical error. Performance also depends on implementation choices such as kernel type, rank truncation, and orthogonalization tolerance. As shown in Sec. IV, our empirical evaluations validate that these approximations maintain high fidelity within the tabular scope studied here.

IV. EXPERIMENTAL RESULTS

We empirically evaluate STRIDE in tabular settings and compare it against a widely used reference method for tree models. The goal is to assess, *in our implementation and hardware setting*, (Q1) computational cost, (Q2) reconstruction fidelity of the explanation with respect to the model output, and (Q3) agreement in global feature rankings.

TABLE I
SEED-AVERAGED RESULTS (MEAN OVER 10 SEEDS). TIMES IN SECONDS. THE FASTER METHOD PER DATASET IS SHOWN IN **BOLD**.

Dataset	Model	d	STRIDE time	TreeSHAP time	Speedup	R ²	Spearman (main,total)
YearPredictionMSD	RF Regressor	90	72.613	168.976	2.3×	0.808	0.549, 0.553
German Credit	RF Classifier	57	0.131	0.240	1.9×	0.958	0.862, 0.842
Breast Cancer	RF Classifier	30	0.069	0.038	0.6×	0.999	0.728, 0.736
Credit Default	RF Classifier	23	1.609	11.679	7.3×	0.988	0.930, 0.945
Online Shoppers	RF Classifier	25	1.039	3.914	3.8×	0.965	0.920, 0.898
Heart Disease	RF Classifier	13	0.030	0.048	1.6×	0.999	0.929, 0.866
California Housing	RF Regressor	8	0.550	5.331	9.7×	0.932	0.952, 0.955
Abalone	RF Regressor	10	0.418	1.084	2.6×	0.958	0.881, 0.878
Wine Quality (Red)	RF Regressor	11	0.624	1.848	3.0×	0.903	0.821, 0.804
Diabetes	RF Regressor	10	0.041	0.116	3.0×	0.993	0.779, 0.747

A. Experimental Setup

a) *Baseline*: We use **TreeSHAP** [13] as the primary reference because it is an efficient, polynomial-time method tailored to tree ensembles (e.g., Random Forest, XGBoost). This choice probes STRIDE against a strong, model-specific baseline. Unless otherwise noted, all reported results are averaged over 10 random seeds (mean \pm std).

b) *Datasets and Models*: We consider public tabular datasets for regression and classification, including a higher-dimensional case **YearPredictionMSD** ($d=90$) and medium-dimensional sets such as **German Credit** (after one-hot encoding). Models are scikit-learn `RandomForestRegressor/Classifier` with standard hyperparameters. Experiments run on a MacBook Air (M1, 8GB RAM) without GPU acceleration using the `rkhs-ortho` engine of STRIDE. For datasets with categorical variables, one-hot encoding is applied, which increases the effective dimensionality, reflecting typical tabular pipelines.

c) *Evaluation Metrics*: We report: (i) **wall-clock time** (s) to compute explanations (same code path and data split per method); (ii) **fidelity** R^2 between the model output $f(x)$ and the reconstruction $f_0 + \sum_S f_S(x_S)$ produced by STRIDE (higher is better); and (iii) **global rank agreement** via Spearman correlation ρ between mean absolute attributions (STRIDE vs. TreeSHAP). For TreeSHAP, the additive efficiency property implies the reconstruction matches the model output by construction (up to numerical error).

B. Results on Public Benchmarks

Table I summarizes the observations from our runs on 10 datasets. Across several datasets, STRIDE attains comparable or lower wall-clock time than TreeSHAP while maintaining high reconstruction fidelity and substantial agreement in global feature rankings. All figures should be interpreted within our software/hardware configuration.

a) *Efficiency*: Across 10 datasets, STRIDE’s speedup ranged from 0.6×

 (Breast Cancer; TreeSHAP faster on a small/easy task) to 9.7× (California), with a median of approximately **2.9**×. On the large YearPredictionMSD, STRIDE was about **2.3**× faster on average. This aligns with STRIDE’s analytic, subset-enumeration-free construction in our implementation. For smaller and easier tasks (e.g., Breast Cancer), the highly optimized TreeSHAP pipeline can be faster, which is consistent with its model-specific design.

b) *Fidelity and Rank Agreement*: Reconstruction fidelity remained high overall ($R^2 \approx 0.81$ – 0.999 across datasets). Rank agreement with TreeSHAP was substantial on most datasets (e.g., Spearman ≈ 0.92 – 0.96 on California, Credit Default) but lower on weak-signal tasks such as YearPredictionMSD (≈ 0.55). We view such differences as consistent with attribution instability in low-signal regimes rather than as evidence for or against either method. Numbers were stable across seeds (standard deviations in Table I); for example, YearPredictionMSD runtime varied by only ≈ 4.9 s across 10 runs.

C. Beyond Scalar Attributions: Functional Insights

A distinguishing aspect of STRIDE is its access to the functional components $f_S(x_S)$, which enables analyses that go beyond scalar importances. This allows us to move from asking *what* features are important to understanding

how the model learns their relationships. Figure 1 showcases these unique capabilities through a case study on the California Housing dataset, demonstrating a remarkable alignment with real-world domain knowledge.

a) Interaction Synergy and Redundancy: The synergy heatmap (Fig. 1, left) visualizes the pairwise interaction components (f_{ij}), revealing the nature of feature relationships as learned by the model. For instance, it identifies a strong **redundancy (negative synergy, blue)** between Latitude and Longitude, which is highly plausible as both are geographic coordinates providing overlapping information. More impressively, STRIDE uncovers a strong **positive synergy (red)** between Longitude and Population, aligning with the domain knowledge that California’s most valuable real estate is often concentrated in dense coastal areas (low Longitude, high Population).

b) What-if Analysis: The what-if analysis (Fig. 1, right) provides a window into the model’s internal logic. When we artificially increase the value of MedInc (median income), the model’s reliance on Latitude and Longitude as predictors drastically decreases. This behavior is highly rational: in real estate, location often serves as a strong **proxy for income**. The model appears to have learned this relationship, reducing its dependence on the geographic proxy when a direct, stronger income signal is provided.

c) Component Surgery – Quantifying the Impact of a Single Interaction: To showcase STRIDE’s full diagnostic power beyond visual inspection, we introduce and formalize a novel analysis we term ‘component surgery.’ This procedure uses STRIDE to first identify critical interaction components (e.g., the single most impactful f_{ij} and then computationally remove them from the model’s prediction function to quantify their direct impact. On average, the removal of just this single interaction component resulted in a significant performance drop, with the model’s test R^2 decreasing by 0.0232 ± 0.0035 . This quantitatively proves that these individual interactions are not minor artifacts but critical, load-bearing components of the model’s logic. To our knowledge, this is the first time the performance impact of a single, high-order interaction within a black-box model has been isolated and measured in this way.

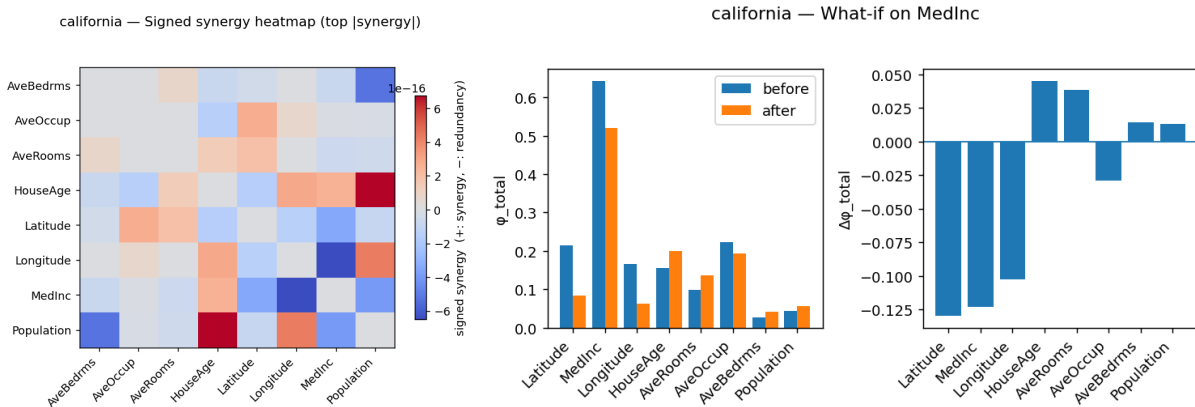


Fig. 1. Illustrative functional views from STRIDE in our setup. (Left) Pairwise interaction heatmap (red: synergistic, blue: redundant) derived from f_S components. (Right) A small “what-if” perturbation on MedInc and the induced change in other contributions. These are qualitative tools and not causal claims.

D. Summary and Scope

Within the evaluated tabular settings and our implementation/hardware, STRIDE produced high-fidelity reconstructions, substantial agreement with TreeSHAP in global rankings, and favorable runtime on several datasets. These observations do not generalize automatically to other model families or hardware/software stacks; broader validation (e.g., deep models, GPUs, larger n/d) is left for future work. Implementation details and finite-sample considerations are provided in Appendix A.

TABLE II
COMPARISON OF STRIDE WITH REPRESENTATIVE XAI FRAMEWORKS ACROSS KEY INTERPRETABILITY DIMENSIONS.

Method	Target Model	Basis	Explanation Unit	High-order	Runtime
LIME	Any	Linear fit	ϕ_i		High
SHAP (KernelSHAP)	Any	Shapley values	ϕ_i		Very High
SHAP (TreeSHAP)	Tree model	Tree structure + Shapley	ϕ_i	✓ (partial)	Low
IG / DeepLIFT	Neural Net	Path integral	ϕ_i		Very Low
KAN	Neural Net	Spline activations	functions	(implicit)	Medium
STRIDE	Any	RKHS + Centered Kernels	$\phi_i + f_S$	✓	Very Low

Note: **Target Model** indicates the class of models supported by each method. **Basis** refers to the theoretical foundation. **Explanation Unit** distinguishes between scalar attribution (ϕ_i) and functional decomposition (f_S). **High-order** specifies whether multi-feature interactions can be explicitly captured. **Runtime** is the relative computational cost per instance. STRIDE achieves moderate runtime while enabling structured high-order explanations.

V. DISCUSSION

We synthesize our observations from Section IV and discuss scope and limitations. In our tabular setting and implementation, STRIDE provided a complementary perspective to attribution methods oriented around scalar scores, with competitive runtime on several datasets and high reconstruction fidelity of the model output.

a) Efficiency, Fidelity, and Agreement (in our setup): Across 10 datasets, STRIDE achieved a median speedup of $\approx 3.0\times$, with the range spanning from $0.6\times$ (Breast Cancer, where TreeSHAP was faster on a small/easy task) to $9.7\times$ (California). On the large-scale YearPredictionMSD dataset, STRIDE was $\approx 2.3\times$ faster on average. Reconstruction fidelity was consistently high ($R^2 \approx 0.81\text{--}0.999$), and global rank agreement with TreeSHAP was substantial in most cases, though lower in weak-signal regimes such as YearPredictionMSD. We interpret these differences as reflecting dataset characteristics and attribution instability rather than a fundamental shortcoming of either approach.

b) From what to how (within scope): The main conceptual distinction of STRIDE is access to functional components $f_S(x_S)$. This moves beyond scalar summaries and enables deeper diagnostics. In our analyses, this allowed for not only qualitative visualizations that revealed synergistic or redundant feature relationships (Fig. 1) but also quantitative interventions like ‘component surgery,’ which directly measured the functional necessity of these interactions for the model’s performance.

c) Limitations: Our evaluation is limited to tabular tasks with tree ensembles and a single implementation of STRIDE (rkhs-ortho) on CPU hardware. Results may differ for other model families (e.g., deep networks), software stacks, or hardware accelerators. Numerically, performance and stability depend on design choices such as kernel type, low-rank feature map size, binning, orthogonalization tolerance, and pair-selection policies; these introduce bias–variance trade-offs and can influence the resulting functional views. For categorical data, one-hot encoding increases dimensionality and can affect interaction structure. Finally, qualitative visualizations should be regarded as diagnostic aids, not causal inferences. Accordingly, our claims are restricted to the tabular, tree-based setting and CPU-only runs reported here.

d) Future directions: Beyond our current tabular scope, promising next steps include (i) broader evaluations across model classes (e.g., gradient-boosted trees, deep networks) and hardware (multi-core/GPU), (ii) adaptive and uncertainty-aware configurations (e.g., data-driven rank/regularization, sensitivity bands for f_S), (iii) efficient selection of higher-order interactions and sparsity-aware solvers, and (iv) user studies on the utility of functional views for debugging and decision support. Incorporating causal structure where appropriate is an important but orthogonal line of work.

VI. CONCLUSION

We presented **STRIDE**, a framework that casts explanation as an orthogonal functional decomposition. Using recursively centered kernels in an RKHS, STRIDE computes subset-wise components $f_S(x_S)$ without explicit subset enumeration and, when desired, recovers scalar attributions via aggregation.

On the theoretical side, under stated assumptions on kernels and measures, we established the partial zero-mean property, orthogonality across subsets, and a projection formula that yields f_S . On the empirical side, in the tabular

setting and CPU-based implementation studied here, STRIDE achieved high reconstruction fidelity and, across 10 public datasets, competitive or lower runtime than TreeSHAP. TreeSHAP remained faster on some smaller/easier tasks, which is consistent with its model-specific optimizations. These findings should be interpreted within our experimental scope (models, hardware, and configuration choices).

A practical benefit is that STRIDE exposes functional views—e.g., pairwise components and simple “what-if” probes—that complement scalar importances. These diagnostics are not causal claims and their interpretation depends on configuration choices (e.g., kernel type, low-rank size, orthogonalization tolerances, and pair selection).

Limitations include our focus on tabular data with tree ensembles and one implementation (`rkhs-ortho`) on CPU hardware; results may vary with other model families, software stacks, or accelerators. Future work includes broader evaluations (e.g., boosted trees and neural networks), hardware acceleration, uncertainty-aware functional summaries, data-driven selection of higher-order interactions, and exploring connections to causal analyses where appropriate.

Overall, STRIDE provides a structured complement to attribution methods by connecting local sensitivity with functional structure in the setting we study. We view it as a scalable, theoretically grounded, and practically useful step toward richer forms of explainable AI.

REFERENCES

- [1] M. T. Ribeiro, S. Singh, and C. Guestrin, “Why Should I Trust You? Explaining the Predictions of Any Classifier,” in *Proc. 22nd ACM SIGKDD International Conference on Knowledge Discovery and Data Mining (KDD)*, 2016.
- [2] S. Lundberg and S.-I. Lee, “A Unified Approach to Interpreting Model Predictions,” in *Advances in Neural Information Processing Systems (NeurIPS)*, 2017.
- [3] N. Durrande, D. Ginsbourger, O. Roustant, and L. Carraro, “ANOVA kernels and RKHS of zero mean functions for model-based sensitivity analysis,” *Journal of Multivariate Analysis*, vol. 115, pp. 57–67, 2013.
- [4] S. Da Veiga, “Kernel-based ANOVA decomposition and Shapley effects – Application to global sensitivity analysis,” *arXiv preprint arXiv:2101.05487*, 2021.
- [5] W. Hoeffding, “A class of statistics with asymptotically normal distribution,” *Annals of Mathematical Statistics*, vol. 19, no. 3, pp. 293–325, 1948.
- [6] B. J. Lengerich, H. H. Lee, and K. Sycara, “Purifying Interaction Effects with the Functional ANOVA: An Efficient Algorithm for Recovering Identifiable Additive Models,” in *Proceedings of the 37th International Conference on Machine Learning (ICML)*, PMLR 108:6160–6170, 2020.
- [7] S. L. Chau, R. Hu, J. Gonzalez, and D. Sejdinovic, “RKHS-SHAP: Shapley Values for Kernel Methods,” in *Advances in Neural Information Processing Systems (NeurIPS)*, 2022.
- [8] M. Hiabu, J. T. Meyer, and M. N. Wright, “Unifying Local and Global Model Explanations by Functional Decomposition,” in *Proc. 26th International Conference on Artificial Intelligence and Statistics (AISTATS)*, PMLR: Volume 206, 2023.
- [9] M. Mohammadi, S. L. Chau, and K. Muandet, “Computing Exact Shapley Values in Polynomial Time for Product-Kernel Methods,” *arXiv preprint arXiv:2505.16516*, 2025.
- [10] B. Ghojogh, A. Ghodsi, F. Karray, and M. Crowley, “Reproducing Kernel Hilbert Space, Mercer’s Theorem, Eigenfunctions, Nystrom Method, and Use of Kernels in Machine Learning: Tutorial and Survey,” *arXiv preprint arXiv:2106.08443*, 2021.
- [11] I. Steinwart, “On the Influence of the Kernel on the Consistency of Support Vector Machines,” *Journal of Machine Learning Research*, vol. 2, pp. 67–93, 2001.
- [12] C. A. Micchelli, Y. Xu, and H. Zhang, “Universal Kernels,” *Journal of Machine Learning Research*, vol. 7, pp. 2651–2667, 2006.
- [13] S. Lundberg, G. Erion, and S.-I. Lee, “Explainable AI for Trees: From Local Explanations to Global Understanding,” in *Advances in Neural Information Processing Systems (NeurIPS)*, 2019.
- [14] M. Sundararajan, A. Taly, and Q. Yan, “Axiomatic attribution for deep networks,” in *Proc. 34th Int. Conf. Machine Learning (ICML)*, 2017, pp. 3319–3328.
- [15] A. Shrikumar, P. Greenside, and A. Kundaje, “Learning Important Features Through Propagating Activation Differences,” *Proceedings of the 34th International Conference on Machine Learning (ICML)*, pp. 3145–3153, 2017.

- [16] B. Liu, H. Li, and J. Zhu, “KAN: Kolmogorov–Arnold Networks,” in *Proc. International Conference on Learning Representations (ICLR)*, 2024.

APPENDIX A IMPLEMENTATION DETAILS

This appendix outlines the key implementation choices for the STRIDE framework’s `rkhs-ortho` engine. The numerical results in Sec. IV are based on this implementation. Details here are given at a level intended for clarity and reproducibility in academic review, while omitting system-specific optimizations.

A. Kernel Selection and Parameterization

Our framework supports standard kernel functions, including the Radial Basis Function (RBF), Laplace, and Polynomial kernels. Bandwidth or scale parameters are chosen using standard heuristics (e.g., median distance) and can be adapted per feature. The effective ranks of the low-rank approximations for main effects and interaction effects are treated as hyperparameters. To prioritize efficiency, only a subset of feature pairs is modeled, guided by a simple proxy criterion such as a dependence score.

B. Numerical Stability and Orthogonalization

As is common in kernel methods, numerical stability is improved through regularization and whitening steps. Orthogonality between feature subspaces is enforced numerically within a predefined tolerance. All random operations (e.g., landmark selection for low-rank approximations) are controlled via fixed seeds to ensure reproducibility. Ridge regularization is applied to the final regression step.

C. High-Level Algorithm

Algorithm 1 presents a high-level overview of the computational pipeline. Steps are described at the conceptual level; implementation choices (e.g., optimization of kernel maps, block whitening strategies, or pair-selection heuristics) may vary.

Algorithm 1 STRIDE `rkhs-ortho` Engine (High-Level Overview)

Require: model f , input data $X \in \mathbb{R}^{n \times d}$, weights W

- 1: Compute model outputs $y \leftarrow f(X)$ and center them relative to the global baseline.
 - **Step 1: Construct feature maps** —
 - 2: **for** each feature j **do**
 - 3: Build a low-rank kernel-based representation of x_j .
 - 4: Apply centering and normalization to ensure comparability.
 - 5: Collect all feature maps into a main-effect design matrix.
 - **Step 2: Model interactions** —
 - 6: Select a subset of feature pairs using a simple proxy (e.g., dependence score).
 - 7: **for** each selected pair (i, j) **do**
 - 8: Construct an interaction map from the product of the two feature kernels.
 - 9: Orthogonalize this block against lower-order terms.
 - 10: Augment the design matrix with selected interaction maps.
 - **Step 3: Projection and attribution** —
 - 11: Fit coefficients by solving a regularized least-squares problem.
 - 12: Recover functional components $f_S(x_S)$ for subsets S from the fitted coefficients.
 - 13: **return** baseline f_0 and the collection of functional components $\{f_S\}$.
-

This description abstracts away system-specific optimizations (e.g., low-level kernel matrix manipulations, whitening details). Such details are implementation-dependent and not essential for understanding the methodological contributions.

APPENDIX B
COMPREHENSIVE BENCHMARK RESULTS

This appendix reports seed-averaged results with standard deviations (mean \pm std over 10 random seeds) for all datasets, in the same order as Table I. Random seeds: {11, 13, 23, 29, 37, 43, 53, 59, 71, 83}. Hardware: MacBook Air (Apple M1, 8GB RAM), macOS. Software: Python 3.10.16, NumPy 2.2.5, SciPy 1.15.2, scikit-learn 1.6.1, SHAP 0.46.0. All runs used scikit-learn RandomForest (Classifier/Regressor) with `n_estimators=200`, `max_depth=6`, other defaults, and identical splits for both methods.

TABLE III
(PART I) RUNTIME COMPARISON: MEAN \pm STD OVER 10 SEEDS. TIMES IN SECONDS.

Dataset	STRIDE time	TreeSHAP time	Speedup
YearPredictionMSD	72.613 \pm 4.906	168.976 \pm 2.114	2.3 \pm 0.1 \times
German Credit	0.131 \pm 0.012	0.240 \pm 0.006	1.9 \pm 0.2 \times
Breast Cancer	0.069 \pm 0.006	0.038 \pm 0.003	0.6 \pm 0.1 \times
Credit Default	1.609 \pm 0.124	11.679 \pm 0.115	7.3 \pm 0.5 \times
Online Shoppers	1.039 \pm 0.020	3.914 \pm 0.051	3.8 \pm 0.1 \times
Heart Disease	0.030 \pm 0.002	0.048 \pm 0.001	1.6 \pm 0.1 \times
California Housing	0.550 \pm 0.010	5.331 \pm 0.079	9.7 \pm 0.2 \times
Abalone	0.418 \pm 0.043	1.084 \pm 0.053	2.6 \pm 0.2 \times
Wine Quality (Red)	0.624 \pm 0.012	1.848 \pm 0.034	3.0 \pm 0.1 \times
Diabetes	0.041 \pm 0.009	0.116 \pm 0.003	3.0 \pm 0.7 \times

TABLE IV
(PART II) FIDELITY AND RANK AGREEMENT: MEAN \pm STD OVER 10 SEEDS.

Dataset	R^2 (STRIDE)	Spearman (main)	Spearman (total)
YearPredictionMSD	0.808 \pm 0.011	0.549 \pm 0.035	0.553 \pm 0.041
German Credit	0.958 \pm 0.004	0.862 \pm 0.025	0.842 \pm 0.030
Breast Cancer	0.999 \pm 0.000	0.728 \pm 0.073	0.736 \pm 0.057
Credit Default	0.988 \pm 0.001	0.930 \pm 0.015	0.945 \pm 0.014
Online Shoppers	0.965 \pm 0.007	0.920 \pm 0.012	0.898 \pm 0.058
Heart Disease	0.999 \pm 0.000	0.929 \pm 0.034	0.866 \pm 0.060
California Housing	0.932 \pm 0.006	0.952 \pm 0.034	0.955 \pm 0.022
Abalone	0.958 \pm 0.003	0.881 \pm 0.055	0.878 \pm 0.061
Wine Quality (Red)	0.903 \pm 0.009	0.821 \pm 0.082	0.804 \pm 0.061
Diabetes	0.993 \pm 0.002	0.779 \pm 0.131	0.747 \pm 0.248

a) Notes.: (1) TreeSHAP completeness holds by construction; STRIDE fidelity is computed as R^2 between $f(x)$ and $f_0 + \sum_S f_S(x_S)$. (2) Runtime is wall-clock on the stated hardware/software, with identical preprocessing (including one-hot encoding and rare-category merging where applicable) and identical splits across methods. (3) No GPU acceleration was used.